

Current Biology

Trigeminal ganglion and sensory nerves suggest tactile specialization of elephants

Highlights

- The elephant trigeminal ganglia are larger than a macaque monkey brain
- The elephant infraorbital nerve innervating the trunk contains 4,00,000 axons
- The elephant infraorbital nerve is thicker than all other sensory nerves
- Elephants might be very tactile animals

Authors

Leopold Purkart, John M. Tuff, Malav Shah, ..., Guido Fritsch, Thomas Hildebrandt, Michael Brecht

Correspondence

michael.brecht@bccn-berlin.de

In brief

Purkart et al. study the trigeminal ganglion and sensory nerves of elephants. The trigeminal ganglia of elephants are enormous. The infraorbital nerve innervating the trunk contains 4,00,000 axons. The infraorbital nerves are thicker than the elephant spinal cord and other sensory nerves. Elephants might be very tactile.



Report

Trigeminal ganglion and sensory nerves suggest tactile specialization of elephants

Leopold Purkart,¹ John M. Tuff,^{1,2} Malav Shah,¹ Lena V. Kaufmann,¹ Carlotta Altringer,¹ Eduard Maier,¹ Undine Schneeweiß,¹ Elcin Tunckol,¹ Lennart Eigen,¹ Susanne Holtze,³ Guido Fritsch,³ Thomas Hildebrandt,^{3,5} and Michael Brecht^{1,4,5,6,*}

¹Bernstein Center for Computational Neuroscience Berlin, Humboldt-Universität zu Berlin, Philippstr. 13, Haus 6, 10115 Berlin, Germany

²Max Planck School of Cognition, Stephanstraße 1A, Leipzig, Germany

³Leibniz Institute for Zoo and Wildlife Research, Alfred-Kowalke-Strasse 17, 10315 Berlin, Germany

⁴NeuroCure Cluster of Excellence, Humboldt-Universität zu Berlin, Berlin, Germany

⁵Senior author

⁶Lead contact

*Correspondence: michael.brecht@bccn-berlin.de

<https://doi.org/10.1016/j.cub.2021.12.051>

SUMMARY

Sensory nerves are information bottlenecks giving rise to distinct sensory worlds across animal species.¹ Here, we investigate trigeminal ganglion^{2,3} and sensory nerves⁴ of elephants. The elephant trigeminal ganglion is very large. Its maxillary branch, which gives rise to the infraorbital nerve innervating the trunk, has a larger diameter than the animal's spinal cord, i.e., trunk innervation is more substantive than connections of the brain to the rest of the body. Hundreds of satellite cells surround each trigeminal neuron, an indication of exceptional glial support to these large projection neurons.^{5–7} Fiber counts of Asian elephant infraorbital nerves of averaged 4,00,000 axons. The infraorbital nerve consists of axons that are ~10 μm thick and it has a large diameter of 17 mm, roughly 3 times as thick as the optic and 6 times as thick as the vestibulocochlear nerve. In most mammals (including tactile specialists) optic nerve fibers^{8–10} greatly outnumber infraorbital nerve fibers,^{11,12} but in elephants the infraorbital nerve fiber count is only slightly lower than the optic nerve fiber count. Trunk innervation (nerves and ganglia) weighs ~1.5 kg in elephant cows. Our findings characterize the elephant trigeminal ganglion as one of the largest known primary sensory structures and point to a high degree of tactile specialization in elephants.

RESULTS AND DISCUSSION

The aim of this investigation was to elucidate the cellular organization of the elephant trigeminal system. The trigeminal ganglion is the location of the cell bodies of the trigeminal nerve, which innervates the face with its mandibular, maxillary, and ophthalmic branch. The maxillary branch is of particular importance in rodents and elephants, where it innervates, via the infraorbital nerve, the facial whiskers and the trunk (the proboscis), respectively. Our data refer to three Asian and five African bush elephants, but not all analyses could be carried out on all specimens (STAR Methods).

The elephant trigeminal ganglion is very large and contains large neurons

The schematic of a trunk-innervating ganglion neuron (red) gives a sense of the size of these cells and their rough position in the elephant's head (Figure 1A). We estimate the length of trunk-tip innervating ganglion cell axons to be round 2.1 m in adult elephant cows, of which about 50 cm run in the skull (until the foramen infraorbitale) and 1.6 m run in the trunk. The elephant trigeminal ganglion is situated at the base of the elephant's skull and is partially encapsulated by bone.

The extracted trigeminal ganglion of the adult Asian elephant cow, Burma, is shown in Figure 1B. The main branches of the

ganglion are labeled. The largest branch is the maxillary, which gives rise to the infraorbital nerve innervating the trunk. Its roughly 2 cm diameter is larger than half of the proximal spinal cord of Burma (Figure 1B, right), i.e., the sensory innervation of the elephant trunk exceeds the connections of the elephant's brain to the elephant's body in neural mass.

A thin (60 μm) Nissl-stained section through the center of a newborn Asian elephant trigeminal ganglion is shown in Figure 1C. The Nissl stain renders ganglion somata in deep blue and massive fiber bundles surround the cell population at the center of ganglion. This alternation of cells and fiber bundles was also seen in the rat trigeminal ganglion⁵ and appears characteristic of many mammals.⁶ Neuronal cells were unusually large. We measured slightly more than 800 neurons from sections in the center of the ganglion and found that they had an average maximal soma diameter of 53 ± 14 (SD) μm (range 20–120 μm) in the baby Asian elephant. In addition, neuronal soma areas were large ($1,402 \pm 793$ SD μm²). These soma sizes were larger than those of the rat trigeminal ganglion (maximum soma diameter: 34.7 ± 10.1 μm [range: 15.3–68.6 μm]; soma area: 662 ± 363 μm² [range: 136–2,225 μm²]). A higher magnification view shows the ganglion cell somata with large neurons surrounded by smaller non-neural (according to NeuN-antibody reactivity) satellite cells (Figure 1D).



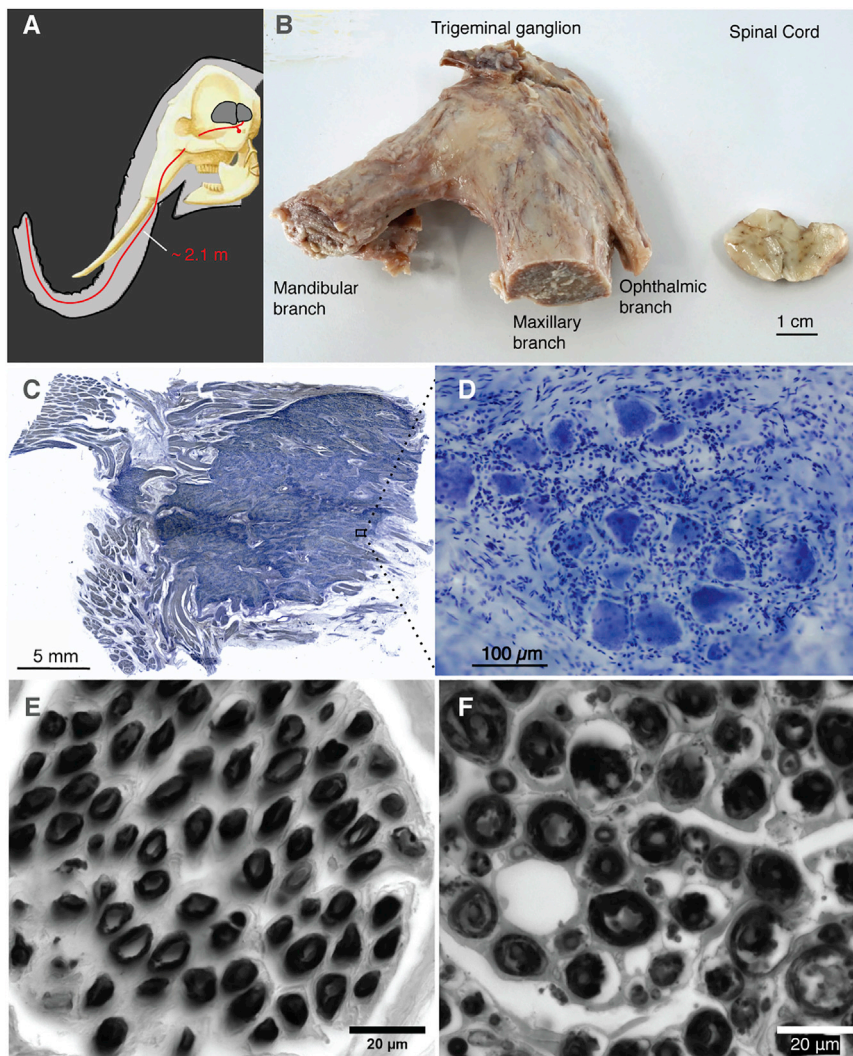


Figure 1. The elephant trigeminal ganglion and infraorbital nerve axons

(A) Schematic of an elephant head with the brain in dark gray and a schematic of a trunk sensory neuron (in red). The neuron's cell body (red circular dot) is situated below the brain in the trigeminal ganglion. (B) Left: the trigeminal ganglion of an adult female Asian elephant (Burma). The ganglion's main sensory branches are labeled and the maxillary branch connects via the infraorbital nerve to the trunk. The trigeminal nerve connecting to the brain stem leaves the ganglion dorsally (opposite from the sensory branches) and has been clipped here. Right: spinal cord of Burma. Note that the maxillary branch is thicker than a hemi-cord, i.e., connections to the trunk are more substantive than the nerve tracts connecting the brain to the body.

(C) A thin (60 μm) Nissl-stained section through the center of the trigeminal ganglion of an Asian baby elephant. Note the alternation of fiber bundles (peripheral) and cells (deep blue, more central).

(D) A higher magnification view of trigeminal ganglion cells. Neuronal cells (large deep blue somata) are surrounded by satellite cells (small round somata). In the upper right corner Schwann cell nuclei (small, deep blue, elongated) can be seen.

(E) A cross-section through the infraorbital nerve of an Asian baby elephant stained with osmium tetroxide to reveal myelin sheets.

(F) Same as in (E) but in this case the infraorbital nerve of an adult Asian elephant (Burma) was stained. Note the slightly larger axon diameters in the adult elephant.

See also [Figure S1](#).

compared to the adult elephants (90.6 ± 42.3 SD μm^2 ; range: 8–245.7 μm^2).

Fiber counts and innervation patterns of elephant infraorbital nerve

As described in detail in [Figure S1](#), there were significantly more satellite cells per trigeminal neuron in elephants (average of 232 in adult animals) than in rats (average of 18 in adult animals, $p = 5.119\text{e}-18$, unpaired, two-tailed Student's *t* test). Satellite cell number is known to increase with cell size.⁷ A plot of satellite cell number against cell soma area revealed that there is a genuinely larger number of satellite cells and a steeper increase of satellite cell number with trigeminal neuron soma area in elephants compared to rats. These findings indicate an extraordinary glial support of the large trigeminal projection neurons in elephants.

Next, we wondered how big the axons of these cells are, and to this end, we stained infraorbital nerve cross-sections with osmium tetroxide. We observed large caliber axons in both baby ([Figure 1E](#)) and adult elephants ([Figure 1F](#)). Axon diameters were smaller in the two baby Asian elephants (maximum diameter: 8.7 ± 1.6 SD μm ; range: 4.8–14.8 μm) than in an adult African and an adult Asian elephant (maximum diameter: 12.4 ± 2.9 SD μm ; range: 4.4–22.1 μm) studied. Similarly, axon cross-sections were smaller in baby Asian elephants (42 ± 14 SD μm^2 ; range: 8.5–95 μm^2)

Furthermore, we wanted to quantitatively assess the sensory connection to the elephant trunk in terms of fiber number. We did so by staining the left and the right infraorbital nerve of a baby Asian elephant with a primary antibody against Neurofilament H, an antibody, which stains all trigeminal sensory axons in other mammals. To this end, we prepared the nerve ([Figure 2A](#)), embedded it in paraffin, and cut thin sections and visualized Neurofilament H reactivity with a secondary antibody coupled to the fluorophore Alexa 488. As in other mammals, the elephant infraorbital nerve showed striking Neurofilament H reactivity ([Figure 2B](#)). A large number of nerve fiber bundles could be distinguished: 338 in the left nerve and 360 bundles in the right nerve of the baby elephant. Individual bundles consisted of numerous nerve fibers ([Figure 2C](#)) and single axons could be readily resolved and counted ([Figure 2D](#)). Because of its size, we did not succeed in staining the entire intact nerve but rather sectioned and stained this nerve specimen in five pieces. We then counted a number of nerve bundles in each of the five pieces and extrapolated a nerve fiber number from the total number of fibers counted—from the cross-sectional

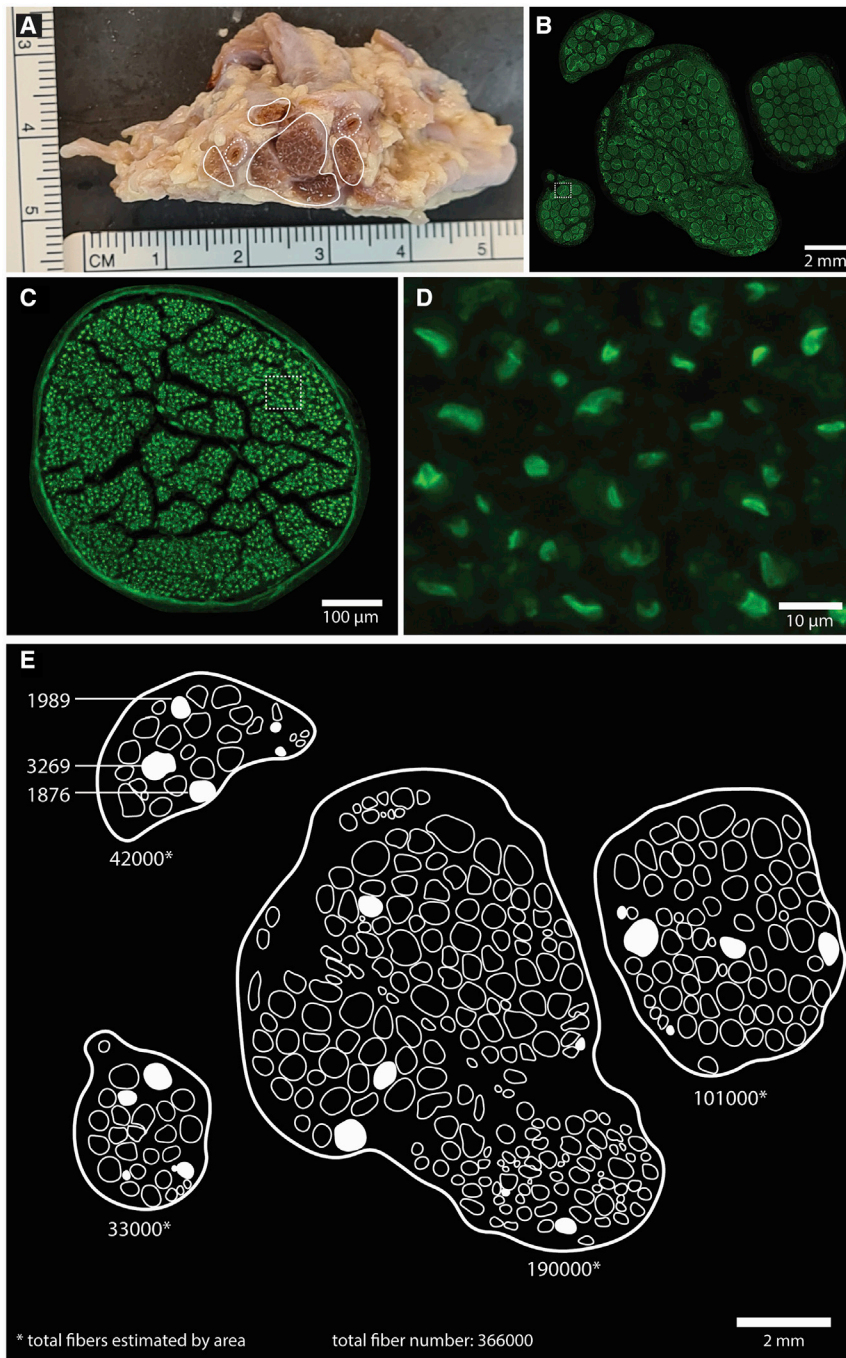


Figure 2. Fiber count of the left infraorbital nerve of a newborn Asian elephant

(A) Cross-section of the elephant infraorbital nerve. Nerve cords are indicated by solid outlines and blood vessels by dashed outlines.

(B) Cross-section of the infraorbital nerve; 338 fiber bundles are revealed by anti-neurofilament-antibody staining (green fluorescence).

(C) High-magnification epifluorescence micrograph of one fiber bundle. Single axon stained by anti-neurofilament antibody can be readily resolved.

(D) Very high-magnification micrograph of single nerve fibers of (C).

(E) Schematic overview of the infraorbital nerve with nerve fiber counts for each nerve segment. Filled circles show fiber bundles that were counted for the assessment of the total fiber number.

See also [Figure S2](#).

elephant infraorbital nerve. If one multiplies the mean axon cross-section area ($\sim 42 \mu\text{m}^2$) that we measured in baby elephants with the number (3,80,000) of fibers, one arrives at a cross-sectional area much smaller than the actual nerve cross-section (see below). Thus, a fair share of the nerve cross-section area is made up of non-neural tissue and space.

We made an effort to determine how the infraorbital nerve innervates the trunk. To this end, we prepared and analyzed micro-CT scans of a baby African elephant trunk. This method allowed us to digitally trace nerves into the trunk, as shown in [Figure S2](#), and suggests the following conclusions: (1) proximally, major branches of the infraorbital nerve run together in the ventrolateral trunk; (2) further branching is observed and thinner branches then innervate more lateral and dorsal trunk territories; (3) nerve branches extend orderly into longitudinal territories with no indication of a cross-over of major branches; (4) nerves systematically get thinner toward the trunk tip, an observation suggestive of “en passant” innervation of trunk tissue; (5) the major share of the infraorbital branches are found on

the ventral side of the trunk; and (6) at least in the proximal parts of the trunk, where nerve branches can be easily and reliably traced, the thinning of nerve branches occurs slowly.

area of counted nerve bundles and from the total area of all nerve bundles in the respective pieces. Cross-section area and fiber count were highly correlated (data not shown). This fiber estimate is schematized in [Figure 2E](#) and it led to an estimate of 3,66,000 axons in the infraorbital nerve shown in [Figure 2](#). The same procedure led to an estimate of 3,95,000 axons in the right nerve of the same baby Asian elephant and to an estimate of 4,45,000 axons in the infraorbital nerve of an adult Asian elephant cow (Burma); averaging these three counts one arrives at an estimate of $\sim 4,00,000$ axons in the Asian

the ventral side of the trunk; and (6) at least in the proximal parts of the trunk, where nerve branches can be easily and reliably traced, the thinning of nerve branches occurs slowly.

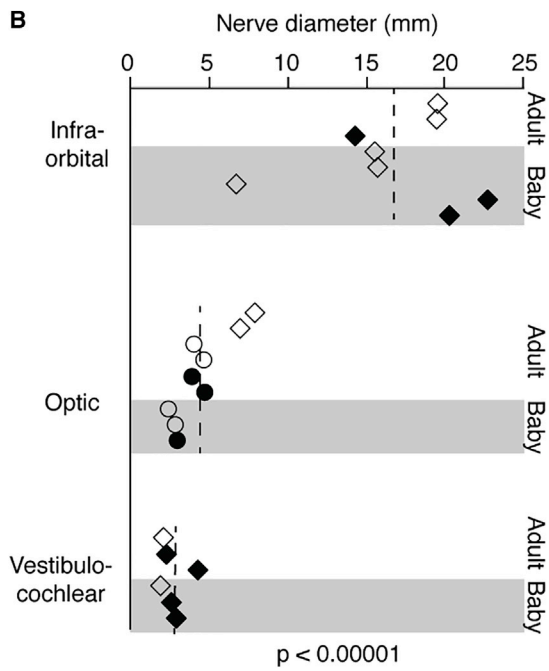
Elephant sensory nerve comparisons

Both trigeminal ganglion size and the very substantial infraorbital nerve fiber counts indicate that the elephant trigeminal system is large; however, elephants are large animals and it may simply be that all nerves of this animal are very large. As a first order assessment of this possibility, we compared elephant sensory

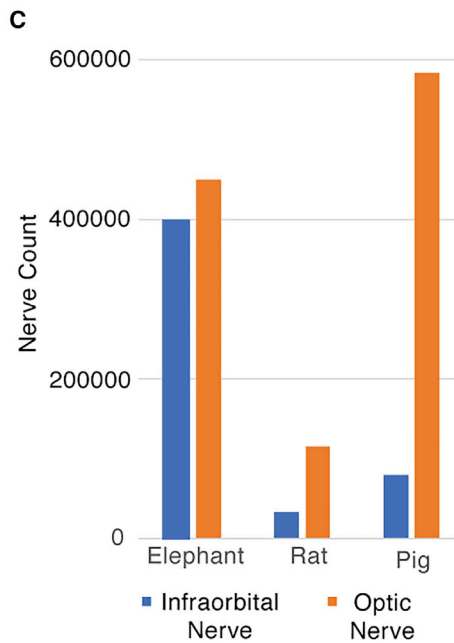
A



B



C



(legend on next page)

nerves. Specifically, we compared the infraorbital nerve (carrying trunk tactile sensory information), the optic nerve (carrying visual information), and the vestibulocochlear nerve (carrying vestibular and auditory information). The differences in diameters of these nerves are notable and the immense infraorbital nerve stands out (Figure 3A). Clearly, not all sensory nerves of the elephant are equally large. Albeit that the number of samples we studied was limited, the nerve thickness differences appeared consistent across Asian and African elephants (Figure 3B); we also plotted the optic nerve data from Kuhrt et al.¹³ for comparison. We show nerve counts from optic nerve and infraorbital nerve from a variety of other studies on other species (Figure 3C). In rats and pigs (both tactile specialists), optic nerve fibers greatly outnumber infraorbital nerve fibers, but in elephants the infraorbital nerve fiber count is only slightly lower than the optic nerve fiber count.

Mass estimates of trigeminal ganglion and infraorbital nerve

The enormous size of the trigeminal ganglion (the specimen shown in Figure 1B) was also reflected in its weight of 54.9 g. This weight overestimates the ganglion weight because of the attached nerve branches, but as we did not correct the weight for fixation-induced shrinkage, the measured weight may not be far off the actual ganglion mass.

We also made estimates of the mass of the infraorbital nerve in adult elephants. To this end, we measured the weight of one segment of the infraorbital nerve of the Asian elephant cow Burma, shown in Figure 3A. We determined a weight of 32 g for the roughly 8 cm long nerve segment. We reasoned that the effects of length shrinkage and weight loss induced by fixation might roughly cancel out, which leads to an estimate of 4 g/cm length of infraorbital nerve in this elephant cow. In an African elephant cow (Zimba), we measured a weight of 60.5 g for a nerve segment roughly 13 cm long, which led to an estimate of 4.65 g/cm length of infraorbital nerve in Zimba. The infraorbital nerve runs in full width for about 50 cm until it reaches the foramen infraorbitale where it branches, yet many of the fibers reach the trunk tip. Assuming the nerve runs at 67% of its width to the tip (a 1.6 m distance), we estimate a weight of approximately ~630 and ~730 g in Burma and Zimba, respectively, for the entire infraorbital nerve. By adding the ganglia and nerve weights we arrive at an estimate of the mass of the elephant trunk innervation: approximately 1.4 and 1.6 kg trunk innervation in the Asian and African elephant cow, respectively.

What do the large trigeminal ganglion and infraorbital nerve tell us about elephant neurobiology?

Elephant trigeminal ganglion

The most conspicuous feature of the elephant trigeminal ganglion is its large size. Given its size, it is surprising that the elephant trigeminal ganglion has barely been studied. The lack

of data is likely related to its buried position at the base of the skull. Our basic observations on ganglion and the infraorbital nerve are similar to those of earlier investigators.^{2,3} Very likely, the large size of elephant trigeminal neurons is related to the long axons they extend. Satellite cells are a special form of supportive glia observed in ganglia⁶ and we suggest that the large number of these cells in elephants is indicative of extraordinary glial support to elephant trigeminal neurons.

Sensory nerve organization and information transmission in different modalities

At first sight, it may seem obvious that elephants have a big infraorbital nerve; however, the details of our data are more complex. For example, why is the elephant infraorbital nerve more than 3 times thicker than the optic nerve (a >13 times larger cross-section), when the elephant optic nerve has a larger fiber count than the elephant infraorbital nerve? We think such differences arise from the much higher temporal precision of tactile fibers compared to visual ones. Visual transduction is based on a G protein-coupled second messenger process,¹⁴ and a temporally precise retinal response to a visual contrast change will have most action potentials in the first 10-ms bin of the response. A temporally precise response to a whisker deflection—directly transduced by mechanosensitive channels—in the rat trigeminal ganglion will have most action potentials in the first 0.1-ms bin of the response.^{15,16} The very thick axons of tactile afferents (such as infraorbital nerve fibers) may be related to the temporal precision of tactile signals. The huge information carrying capacity of tactile afferents¹⁷ may also help in the understanding how a rat can be a more tactile than visual animal (with a somatosensory cortex several times larger than the visual cortex¹⁸ even though its optic nerve fibers greatly outnumber the tactile afferents. We conclude that elephants have unusually many tactile afferents, both in relative terms (compared the optic nerve) and in absolute number.

Trigeminal signaling may impose significant metabolic cost

The energy consumption of individual trigeminal trunk neurons cannot be measured directly in elephants. Two types of costs may be expected: first, action potential propagation will be expensive in these neurons because of their large diameter and great length. The major energetic cost imposed by action potential propagation results from sodium inflow,¹⁹ which is proportional to the exposed surface of the neuron and hence will increase with the square of the axon diameter. Because the axon diameter of infraorbital nerve fibers (~10 μm) is much larger than rodent cortical neuron axons (0.1–0.5 μm), one can expect very high costs. Myelination will reduce such costs in complex ways but will not change the increase of costs with axon length or the steep rise of costs with axon diameter. Second, neural maintenance costs will also be high for these neurons because

Figure 3. Elephant sensory nerves

(A) Sensory nerves of the adult Asian elephant Burma.

(B) Sensory nerve diameters in Asian (empty symbols) and African (filled symbols) elephants. Means per nerve type are indicated as dashed lines. Diamonds refer to our measurements and round symbols refer to optic nerve measurements as reported by Hanani.⁶ Data from adult and newborn elephants separated according to shading. The p value refers to comparison of the diameters of the three nerves by an ANOVA.

(C) Nerve fiber counts from the infraorbital nerve of the elephant, the rat,¹¹ and the domestic pig¹² and the optic nerve of the elephant,¹³ the rat,⁹ and the pig.¹⁰

of their large axon diameter and length. Elephants might rely very strongly on tactile information.

The sensory nerve comparisons and the size of the trigeminal ganglion indicate that elephants might rely very strongly on tactile information. We realize that such a conclusion cannot be made on the basis of a single study and we agree that our data should be interpreted with caution. Nevertheless, even the human retina—arguably one of the most impressive sensory structures—with its ~ 10 cm² area²⁰ and its ~ 0.25 mm thickness,²¹ i.e., a ~ 0.25 g mass, seems small in comparison to the ~ 50 g trigeminal ganglion described here. We lack information for assessing the sensory abilities of elephants. Highly knowledgeable investigators talk about an “excellent” sense of hearing versus a “very good” sense of touch in elephants.²² Similarly, a recent comparative review of the sensory abilities of the Proboscidae devotes more space to elephant hearing than to elephant touch.²³ We note that the infraorbital nerve is more than 6-times thicker than the vestibulo-cochlear nerve (an ~ 37 times larger cross-section). Thus, our data entertain the possibility that elephant touch is truly extraordinary. Elephant trunks contain an enormous number of muscles²⁴ and anatomical analysis revealed numerous tactile specializations of the elephant trunk, in particular with respect to the trunk fingers.²⁵ Ultimately, behavioral assays will be necessary to tell us how tactile, visual, olfactory, etc. an animal is, and to what extent such categorizations are meaningful. Behavioral studies have also suggested a high degree of tactile sensitivity of the elephant trunk.²⁶ Elephants constantly touch their environment with their trunk. While such behaviors seem to be of manipulative character to the human eye, these behaviors might well also serve an important sensory function.

STAR★METHODS

Detailed methods are provided in the online version of this paper and include the following:

- **KEY RESOURCES TABLE**
- **RESOURCE AVAILABILITY**
 - Lead contact
 - Materials availability
 - Data and code availability
- **EXPERIMENTAL MODEL AND SUBJECT DETAILS**
 - Elephant specimens
 - Rat specimens
- **METHOD DETAILS**
 - Elephant preparation, ganglion/nerve collection and nerve measurements
 - Nerve and ganglion preparation and staining
 - Osmium tetroxide stain
 - Cellular and axon size measurements
 - Microfocus computed tomography
- **QUANTIFICATION AND STATISTICAL ANALYSIS**
 - Statistical analysis

SUPPLEMENTAL INFORMATION

Supplemental information can be found online at <https://doi.org/10.1016/j.cub.2021.12.051>.

ACKNOWLEDGMENTS

The study was supported by BCCN Berlin, Humboldt-Universität zu Berlin, the Deutsche Forschungsgemeinschaft (DFG, German Research Foundation) under Germany’s Excellence Strategy—EXC-2049—390688087, the BMBF, and Max Planck Society. We thank Francisca Egelhofer and Aniston Sebastianpillai for their decisive help in brain extraction. Many others also contributed to this paper including Uta Westerhüs, Anne Nessler, Karin Risse, Jana Petzold, Jörg Geiger, and Kristin Mahlow. We also thank Dr. Claudia Szentiks, Zoltan Mezö, Marc Gölkel, and Katharina Brehm for their help with necropsy. Several zoological institutions contributed material to this study, in particular the Zoo Augsburg (Germany), Opel-Zoo (Germany), and Zoo Poznań (Poland).

AUTHOR CONTRIBUTIONS

Conceptualization, L.P., T.H., and M.B.; methodology, L.P., T.H., S.H., L.V.K., E.T., U.S., E.M., G.F., L.E., and M.B.; investigation, L.P., J.M.T., T.H., S.H., L.V.K., E.T., U.S., E.M., M.S., C.A., and M.B.; formal analysis, M.B.; visualization, L.P., L.E., J.M.T., and M.B.; writing, L.P., J.M.T., and M.B.; supervision, M.B.; funding acquisition, M.B.

DECLARATION OF INTERESTS

The authors declare no competing interests.

Received: October 5, 2021

Revised: December 17, 2021

Accepted: December 17, 2021

Published: January 20, 2022

REFERENCES

1. Niven, J.E., and Laughlin, S.B. (2008). Energy limitation as a selective pressure on the evolution of sensory systems. *J. Exp. Biol.* *211*, 1792–1804.
2. Bucciante, L. (1926). La struttura del ganglio di Gasser di elefante. *Arch. Ital. Anat. Embriol.* *23*, 691–707.
3. Sprinz, R. (1952). The innervation of the trunk of the Indian elephant. *Proc. Zool. Soc. Lond.* *122*, 621–624.
4. Nabavizadeh, A., and Reidenberg, J.S. (2019). Anatomy of the proboscideal nerve in the proboscis of the African Elephant (*Loxodonta africana*). *FASEB J.* *33*, 1b148.
5. Legradi, A., Dulka, K., Jancsó, G., and Gulya, K. (2020). Orofacial skin inflammation increases the number of macrophages in the maxillary sub-region of the rat trigeminal ganglion in a corticosteroid-reversible manner. *Cell Tissue Res.* *382*, 551–561.
6. Hanani, M. (2005). Satellite glial cells in sensory ganglia: from form to function. *Brain Res. Brain Res. Rev.* *48*, 457–476.
7. Pannese, E., Ventura, R., and Bianchi, R. (1975). Quantitative relationships between nerve and satellite cells in spinal ganglia: an electron microscopic study. II. Reptiles. *J. Comp. Neurol.* *160*, 463–476.
8. Stone, J., and Halasz, P. (1989). Topography of the retina in the elephant *Loxodonta africana*. *Brain Behav. Evol.* *34*, 84–95.
9. Forrester, J., and Peters, A.A. (1967). Nerve fibres in optic nerve of rat. *Nature* *214*, 245–247.
10. Garcá, M., Ruiz-Ederra, J., Hernández-Barbáchano, H., and Vecino, E. (2005). Topography of pig retinal ganglion cells. *J. Comp. Neurol.* *486*, 361–372.
11. Jacquin, M.F., Hess, A., Yang, G., Adamo, P., Math, M.F., Brown, A., and Rhoades, R.W. (1984). Organization of the infraorbital nerve in rat: a quantitative electron microscopic study. *Brain Res.* *290*, 131–135.
12. Ritter, C., Maier, E., Schneeweiß, U., Wölk, T., Simonnet, J., Malkawi, S., Eigen, L., Tunckol, E., Purkart, L., and Brecht, M. (2021). An isomorphic three-dimensional cortical model of the pig rostrum. *J. Comp. Neurol.* *529*, 2070–2090.

13. Kuhrt, H., Bringmann, A., Härtig, W., Wibbelt, G., Peichl, L., and Reichenbach, A. (2017). The retina of Asian and African elephants: comparison of newborn and adult. *Brain Behav. Evol.* **89**, 84–103.
14. E.R. Kandel, J.H. Schwartz, T.M. Jessell, S. Siegelbaum, A.J. Hudspeth, and S. Mack, eds. (2000). *Principles of Neural Science*, 4 (McGraw-Hill), pp. 1227–1246.
15. Jones, L.M., Depireux, D.A., Simons, D.J., and Keller, A. (2004). Robust temporal coding in the trigeminal system. *Science* **304**, 1986–1989.
16. Bale, M.R., Campagner, D., Erskine, A., and Petersen, R.S. (2015). Microsecond-scale timing precision in rodent trigeminal primary afferents. *J. Neurosci.* **35**, 5935–5940.
17. Arabzadeh, E., Panzeri, S., and Diamond, M.E. (2006). Deciphering the spike train of a sensory neuron: counts and temporal patterns in the rat whisker pathway. *J. Neurosci.* **26**, 9216–9226.
18. Zilles, K., and Wree, A. (1995). Cortical areas. In *The Rat Nervous System*, G. Paxinos, ed. (Academic Press), pp. 649–685.
19. Alle, H., Roth, A., and Geiger, J.R. (2009). Energy-efficient action potentials in hippocampal mossy fibers. *Science* **325**, 1405–1408.
20. Drasdo, N., and Fowler, C.W. (1974). Non-linear projection of the retinal image in a wide-angle schematic eye. *Br. J. Ophthalmol.* **58**, 709–714.
21. Sigelman, J., and Ozanics, V. (1982). Retina. In *Ocular Anatomy, Embryology and Teratology*, A. Jacobiec, ed. (Harper & Row).
22. Shoshani, J., Kupsky, W.J., and Marchant, G.H. (2006). Elephant brain. Part I: gross morphology, functions, comparative anatomy, and evolution. *Brain Res. Bull.* **70**, 124–157.
23. Moore, A.M., Hartstone-Rose, A., and Gonzalez-Socoloske, D. (2021). Review of sensory modalities of sirenians and the other extant Paenungulata clade. *Anat. Rec. (Hoboken)*. Published online August 23, 2021. <https://doi.org/10.1002/ar.24741>.
24. Cuvier, G., and Dumeril, A.M. (1838). *Lecons d'anatomie comparée: 2* (Societe Typographique Belge).
25. Rasmussen, L.E.L., and Munger, B.L. (1996). The sensorineural specializations of the trunk tip (finger) of the Asian elephant, *Elephas maximus*. *Anat. Rec.* **246**, 127–134.
26. Dehnhardt, G., Friese, C., and Sachser, N. (1997). Sensitivity of the trunk of Asian elephants for texture differences of actively touched objects. *Z. Saugetierkd* **62**, 37–39.
27. Rasenberger, S. (2019). Das zentrale auditorische system und dessen neuronale extrazelluläre Matrix bei Elefant (*Elephas maximus*, *Loxodonta africana*) und Klippschliefer (*Procavia capensis*) als Vertreter der Afrotheria. <https://core.ac.uk/download/pdf/226140675.pdf>.
28. Manger, P.R., Pillay, P., Maseko, B.C., Bhagwandin, A., Gravett, N., Moon, D.J., Jillani, N., and Hemingway, J. (2009). Acquisition of brains from the African elephant (*Loxodonta africana*): perfusion-fixation and dissection. *J. Neurosci. Methods* **179**, 16–21.
29. Shoshani, J. (1982). On the dissection of a female Asian elephant (*Elephas maximus* Linnaeus, 1758) and data from other elephants. *Elephant* **2**, 3–93.
30. Purkart, L., Sigl-Glöckner, J., and Brecht, M. (2020). Constant innervation despite pubertal growth of the mouse penis. *J. Comp. Neurol.* **528**, 2269–2279.
31. Metscher, B.D. (2009). MicroCT for comparative morphology: simple staining methods allow high-contrast 3D imaging of diverse non-mineralized animal tissues. *BMC Physiol.* **9**, 11.
32. Metscher, B.D. (2009). MicroCT for developmental biology: a versatile tool for high-contrast 3D imaging at histological resolutions. *Dev. Dyn.* **238**, 632–640.

STAR★METHODS

KEY RESOURCES TABLE

REAGENT or RESOURCE	SOURCE	IDENTIFIER
Antibodies		
Neurofilament H, Chicken polyclonal	Milipore	Cat#: AB5539; RRID: AB_11212161
Alexa Fluor 488 Goat anti-chicken	Thermo Fisher Scientific	Cat#: A-11039; RRID: AB_2534096
Rabbit anti-neuronal nuclei I (NeuN)	Merck	Cat#: ABN78A4; Lot Nr.: 3209767; RRID: AB_10920751
Alexa Fluor 546 donkey anti-mouse	Invitrogen	Cat# Nr.: A10036; Lot Nr.: 1977695; RRID: AB_2534012
Alexa Fluor 488 donkey anti-rabbit	Invitrogen	Cat# Nr.: A21206; RRID: AB_2535792
Chemicals, peptides, and recombinant proteins		
Fluoromount	Biozol	Cat# Nr.: SBA-0100-35
Osmiumtetroxide 4%	SERVA	Cat# Nr.: 31253.02
Eukitt	Sigma-Aldrich	Cat# Nr.: 03989-100ML
Deposited data		
Raw figure image files and a 3D surface model of microCT scan of the African baby elephant trunk	GIN	https://gin.g-node.org/elephant/Purkart
Experimental models: Organisms/strains		
African elephants, <i>Loxodonta africana</i>	IZW-collection from various Zoos	N/A
Asian elephants, <i>Elphas maximus</i>	IZW-collection from various Zoos	N/A
Rat: RjOri:LE	Janvier Labs	https://www.janvier-labs.com/
Software and algorithms		
Adobe Photoshop 2022	Adobe Systems, San Jose, California, USA	https://www.adobe.com/de/products/photoshop.html
AmiraZIBedition 2021	Zuse Institute Berlin, Germany	https://amira.zib.de/download.html
Stereoinvestigator NeuroLucida Neuroexplorer	MBF Bioscience, Williston, USA	https://www.mbfbioscience.com
ImageJ	NIH	https://imagej.nih.gov/ij/notes.html
Other		
Olympus BX51 microscope	Olympus, Japan	https://www.olympus-lifescience.com
YXLON FF 85 CT	YXLON International GmbH, Hamburg, Germany	https://www.yxlon.de/de/products/rontgen-und-ct-prufsysteme/yxlon-ff85-ct

RESOURCE AVAILABILITY

Lead contact

Further information and requests for resources and reagents should be directed to and will be fulfilled by the lead contact, Michael Brecht (michael.brecht@bccn-berlin.de)

Materials availability

This study did not generate new unique reagents

Data and code availability

- All data reported in this paper will be shared by the lead contact and key data are available under: <https://gin.g-node.org/elephant/Purkart>

- This paper does not report original code.
- Any additional information required to reanalyze the data reported in this paper is available from the lead contact upon request.

EXPERIMENTAL MODEL AND SUBJECT DETAILS

Elephant specimens

We worked with a variety of elephant specimens in our study. All specimens came from zoo elephants and were collected by the IZW (Leibniz Institute for Zoo and Wildlife Research, Berlin) over the last three decades in agreement with CITES regulations. All animals included in the study died of natural causes or were euthanized by experienced zoo veterinarians for humanitarian reasons, because of insurmountable health complications.

*Asian elephants, *Elphas maximus**

Data from two newborn Asian elephant babies, which died around birth, were included. In one of them we had access only to the animal's head but not the brain. The brain of this animal was described in a study by Rasenberger.²⁷ We also included data from the adult Asian elephant cow Burma (52 years old) from the Augsburg Zoo.

*African elephants, *Loxodonta africana**

Data from two newborn African elephant babies, which died around birth, were included. In one of them we had access only to half of the head. We also included data from three adult African elephant cows Aruba (41 years old) from Opel-Zoo Kronberg Germany, Zimba (39 years old) from Opel-Zoo Kronberg Germany, and Linda (35 years old) from the Zoo Poznan Poland.

Specimen status

Specimen status varied widely in our study. Most heads or other material reached us frozen and none of the elephant heads/brains were perfused. Even though many of the animals included were dissected by professional veterinarians, the preservation of material varied across specimens. A variety of reasons contribute to a suboptimal preservation of elephant material. Specifically, it often takes days to dissect elephants and the animals' carcasses cool down only very slowly. Furthermore, the freezing leads to freezing artifacts and even in extracted brains fixative action is slow, because of elephant brain size. Some of these problems are discussed and have been partially solved in the following references.^{28,29}

Rat specimens

For comparison we also studied five trigeminal ganglia of adult rats. The organ collection was allowed under a killing permit for rats T HU - 01/20 by Humboldt University. Treatment of rat and elephant samples was identical if not noted otherwise.

METHOD DETAILS

Elephant preparation, ganglion/nerve collection and nerve measurements

Elephant preparation

Heads of deeply frozen baby elephants were removed at the IZW (Leibniz Institute for Zoo and Wildlife Research, Berlin). In adult elephants, heads and trunks were removed at the respective zoos and the remaining skull was trimmed with motorized saws and axes at the IZW Berlin. Brains of baby elephants (after thawing) and brains from trimmed skulls of adult elephants were extracted by Francisca Egelhofer and Aniston Sebastianpillai at the Neuropathology of the Charité, Berlin.

Trigeminal ganglion collection

The way the elephant trigeminal ganglia were collected depended on the way that the elephant brain was removed. In cases, where the brain was collected together with the dura, the trigeminal ganglia (or large parts of them) were contained in the dura on the ventral side of the brain. In one case we removed elephant brain without the dura, which left the trigeminal ganglion remaining at the base of the skull. In this case, we removed additional parts of the skull, which partially encapsulated the ganglion. This procedure led to a more complete collection of the ganglion and this is also the case we show in [Figure 1](#). Altogether, we collected 8 trigeminal ganglia, two from an Asian baby elephant, two from an African baby elephant, two from an adult Asian elephant cow (Burma) and two from an adult African elephant cow (Linda).

Nerve collection

Infraorbital nerves were collected from elephant skulls, where the nerve leaves the foramen infraorbitale. We figured that it was easiest to find the foramen infraorbitale by carefully detaching the trunk tissue/muscle fascia from the os nasale and dissecting from the rostral end of the bone in caudal direction until the foramen infraorbitale became visible. Optic nerves were removed from the skull by opening the bone canal anterior to the optic chiasm. Vestibulocochlear nerves were collected either from the bone canal in the ventral temporal skulls or directly from the brain stem.

Nerve measurements

We visually identified intact nerve parts and determined the minimal and maximal thickness of the nerve. Both minimal and maximal thickness were measured with a caliper independently by two investigators and measurements were averaged; we report the mean of the minimal and maximal thickness in our [Figure 3](#).

Nerve and ganglion preparation and staining

Preparation and staining procedures of the infraorbital nerve were performed analogous to Ritter et al.¹² and Purkart et al.³⁰ In brief, we dissected the infraorbital nerve from the head of a deceased elephant baby, embedded it in paraffin and stained 8 μm cross-sections with a primary antibody against Neurofilament H (Chicken polyclonal, Millipore Cat# AB5539, RRID: AB_11212161). Detection of the antibody signal was performed with a secondary antibody, coupled to the fluorophore Alexa 488 (Goat anti-chicken: Thermo Fisher Scientific Cat# A-11039, RRID: AB_2534096). Z-stacks were taken on a Leica DM5500B epifluorescence microscope with a $\times 63$ oil lens (axial resolution 0.772 μm). The z-planes were 0.1 and 1 μm apart. The images obtained were from 1600 \times 1200 to 8696 \times 7706 pixels in size with a field of view between 203 \times 152 μm and 1103 \times 977 μm . Stacks were analyzed using ImageJ (RRID: SCR_003070).

Ganglia were treated similar to nerve tissue with the exception that thicker sections were cut (40 to 60 μm thickness) and were also stained for Nissl-substance. Another series of 20 μm thick ganglion sections was stained for neuronal somata with rabbit anti-neuronal nuclei I (NeuN) antibody (Merck, Catalog Nr. ABN78A4, Lot Nr. 3209767, RRID: AB_10920751), which we used at a dilution of 1:1000. Series of sections were processed, alternating with Nissl and antibody staining. Sections were processed for NeuN antibody stains. Briefly, sections were incubated in a blocker of 0.1 M PBS, pH 7.2, with 0.5 % Triton X-100 and 5 % normal horse serum for an hour at room temperature before incubation in their respective primary antibodies (see description in text) in the blocker for 48h at 4 $^{\circ}\text{C}$. After rinsing, the sections were incubated in the blocker containing secondary donkey anti-mouse antibody conjugated to Alexa Fluor 546 (1:200; Invitrogen, Catalogue Nr. A10036, Lot Nr. 1977695, RRID: AB_2534012) and secondary donkey anti-rabbit antibody conjugated to Alexa Fluor 488 (1:200; Invitrogen, Catalogue Nr. A21206, RRID: AB_2535792) overnight. The next day sections were washed, mounted and then coverslipped with mounting medium (Fluoromount; Biozol, Eching, Germany, Catalogue Nr. SBA-0100-35).

Osmium tetroxide stain

In order to assess the axon diameter and to verify counts of myelinated fibers in the infraorbital nerve, osmium tetroxide myelin stains were performed on tissue segments, directly before paraffin embedding. For this purpose, sections of the infraorbital nerve of approximately 5 mm width were placed in 2% osmium tetroxide solution (Osmiumtetroxide 4%, SERVA Catalogue Nr. 31253.02) for 1h under constant shaking. After several washing steps with ddH₂O to remove residual staining solution, the nerve segments were embedded in paraffin, cut into 8 μm thick cross-sections and mounted on Carl Roth Adhesion slides Superfrost Plus Gold. The slides were stored overnight in a furnace at 45 $^{\circ}\text{C}$. The following day, sections were deparaffinized in xylol, isopropanol and 100 % ethanol and covered with Eukitt mounting medium (Catalogue Nr. 03989-100ML, Sigma-Aldrich).

Cellular and axon size measurements

Thin Nissl or osmium tetroxide stained sections were viewed with StereoInvestigator software (MBF Bioscience, Williston, USA) employing an Olympus BX51 microscope (Olympus, Japan) with a MBFCX9000 camera (MBF Bioscience, Williston, USA) mounted on the microscope. The microscope was equipped with a motorized stage (LUDL Electronics, Hawthorne, USA) and a z-encoder (Heidenhain, Schaumburg, USA). StereoInvestigator software was used for stereological procedures, cell size and axon diameter measurement and for acquiring images. Digitized images were adjusted for brightness and contrast using Adobe Photoshop (Adobe Systems, San Jose, Calif., USA), but they were not otherwise altered.

Microfocus computed tomography

We used diffusible iodine-based contrast enhanced computed tomography (diceCT) to analyze and visualize nerves in the elephants trunk. To enhance the contrast for microCT the trunk was treated as follows: 30 days in 1% iodine in water, 30 days in 2% iodine in water, 30 days in 3% iodine in water.^{31,32} The trunk was subsequently scanned at the Museum für Naturkunde Berlin with a YXLON FF 85 CT (YXLON International GmbH, Hamburg, Germany). Scans were performed with an isotropic voxel size of 50 μm .

Images were visualized and segmented using an extended version of the Amira software (AmiraZIBedition 2021, Zuse Institute Berlin, Germany). Segmentation was done manually with a combination of the 'Threshold', 'Brush' and 'Lasso' module. Cross-sectional areas were created in Amira with the 'Slice' module and then measured in Adobe Photoshop 2022 (Adobe Systems, San Jose, California, USA) using the 'Magic Wand' tool.

QUANTIFICATION AND STATISTICAL ANALYSIS

Statistical analysis

Nerve diameters of different sensory nerve were compared by an ANOVA (Analysis of variance) and was computed using an online tool (<https://www.socscistatistics.com/tests/anova/default2.aspx>).